Available online at www.sciencedirect.com
ScienceDirect
C. R. Physique 9 (2008) 947–962
COMPTES RENDUS PHYSIQUE
http://france.elsevier.com/direct/COMREN/

Recent advances in optical telecommunications / Avancées récentes en télécommunications optiques

Unified analysis of weakly-nonlinear dispersion-managed optical transmission systems using a perturbative approach

Alberto Bononi *, Paolo Serena, Marco Bertolini

University of Parma, Department of Information Engineering, V.le G. Usberti 181/A, 43100 Parma, Italy

Available online 28 November 2008

Abstract

We provide a unified theoretical framework based on a regular perturbation analysis, capable of both explaining most known results, and of deriving new ones, on system optimization in dispersion-managed long-haul terrestrial optical transmission systems with small-to-moderate nonlinearity. ***To cite this article: A. Bononi et al., C. R. Physique 9 (2008).***

Résumé

Analyse unifiée des systèmes de transmissions optiques gérés en dispersion de non-linéarité faible basée sur une approche perturbative. Nous proposons une représentation théorique unifiée, basée sur une analyse perturbative régulière des équations non-linéaires de propagation des systèmes de transmissions optiques gérés en dispersion, dans le cadre d'un régime de non-linéarité faible à modérée. Cette représentation permet d'expliquer la plupart des résultats connus, et d'obtenir de nouvelles règles en matière d'optimisation des systèmes optiques terrestres de longue portée. ***Pour citer cet article : A. Bononi et al., C. R. Physique 9 (2008).***

Keywords: Optical communications; Dispersion management; NLSE; WDM; Kerr effect

Mots-clés : Communications optiques ; Gestion de dispersion ; ESNL ; WDM ; Effet Kerr

1. Introduction

Long-haul, high bit-rate fiber optic links and networks are today the backbone of the Internet physical infrastructure. Large optical powers are needed for such long-distance communications over many wavelength division multiplexed (WDM) channels, in order to overcome the accumulation of optical noise generated by optical amplifiers. Hence the optical medium becomes nonlinear. The mitigation of optical nonlinearity and chromatic dispersion is the objective of the so-called dispersion-managed (DM) optical transmissions [1]. A typical DM WDM terrestrial link is composed of a bank of modulated lasers, multiplexed onto a pre-compensation fiber and boosted to high power for transmission along a line of N possibly different spans, each composed of a long transmission fiber (typically between 50 and 100 km depending on the application), with in-line compensation, typically implemented by a dispersion com-

* Corresponding author.
E-mail address: alberto.bononi@unipr.it (A. Bononi).

1631-0705/$ – see front matter
doi:10.1016/j.crhy.2008.10.017

pensating fiber within a dual-stage amplifier that recovers the span losses, and with a final post-compensating fiber at the receiver [2]. Many empirical design rules for terrestrial DM systems, sometimes explained by ad-hoc elementary analytical models, have been established after years of experimentation and simulation [3–8]. It is the purpose of this article to show that these design rules, applicable to weakly nonlinear DM systems, can be readily and intuitively explained within a single framework based on a regular perturbation analysis. Such a framework is the result of our original synthesis of several previous studies [9–11,16,15,12–14], mostly inspired by the work of Ablowitz on the so-called DM nonlinear Schrödinger equation (DM-NLSE) for periodic DM systems [16,15], and by the work of Wei [14] which effectively exploited a variational approach proposed in [17,18] that allows the DM-NLSE to be extended to nonperiodic DM links, such as those used in today's heterogeneous optical networks.

The paper is organized as follows. Section 2 gives a brief introduction to the nonperiodic DM-NLSE and its DM kernel [14]. Section 3 extends the study of the first-order logarithmic perturbation (LP1) of Forestieri et al. [20,19] to the present DM case. Section 4 extends Wei's time-domain DM kernel analysis by using probability theory tools that facilitate comprehension of a widely-used pre-compensation optimization rule [6–8]. Section 5 exploits the LP1 solution to derive a new post-compensation optimization rule. Section 6 extends the work of [14,16,21] by giving novel results on inter-pulse interactions in quasi-linear DM systems [22]. Finally, Section 7 extends the nonperiodic DM-NLSE to the WDM case, and derives new and most general expressions of the cross-phase modulation (XPM) filters originally introduced in [23,24].

2. Single-channel DM-NLSE

The nonlinear Schrödinger equation (NLSE) for a *single channel* $A(z,t)$ (in $\sqrt{W}$) propagating along a single-mode fiber optic link in the retarded normalized time t (physical time, normalized to the symbol interval T, in a frame moving at the group velocity, where $R = 1/T$ is the baud rate of the transmitted digital signal) can be written in the engineering notation and in the Fourier transform domain as [25]:

$$\frac{\partial \tilde{A}(z,\omega)}{\partial z} = \frac{g - j\omega^2\beta_2 R^2}{2}\tilde{A}(z,\omega) - j\gamma \iint_{-\infty}^{\infty} \tilde{A}(z,\omega+\omega_1)\tilde{A}(z,\omega+\omega_2)\tilde{A}^*(z,\omega+\omega_1+\omega_2)\frac{\mathrm{d}\omega_1}{2\pi}\frac{\mathrm{d}\omega_2}{2\pi} \tag{1}$$

where for any function $g(t)$ we define its Fourier transform (with engineering sign convention) as $\tilde{g}(\omega) = \int_{-\infty}^{\infty} g(t)\mathrm{e}^{-j\omega t}\,\mathrm{d}t$, where j is the imaginary unit, $\omega = 2\pi f$, with f the frequency normalized to the baud rate; where $g(z)$ is the net gain/attenuation coefficient per unit length, $\beta_2(z)$ is the group velocity dispersion (GVD) coefficient, $\gamma(z)$ is the nonlinear coefficient, and all such parameters are z-varying functions, with span k ending at coordinate z_k, $k = 1,\ldots,N$. In the following, we will define the average of any function $f(z)$ over the interval $[0,z]$ as $\langle f\rangle_z \triangleq \frac{1}{z}\int_0^z f(s)\,\mathrm{d}s$. When z equals the total link length L we will simply write $\langle f\rangle_L \equiv \langle f\rangle$. The function

$$G(z) = \mathrm{e}^{\int_0^z g(s)\,\mathrm{d}s} = \mathrm{e}^{z\langle g\rangle_z}, \qquad G(0) = 1$$

is the net line power gain from 0 to z. Hence $G(z) = \frac{P(z)}{P(0)}$, where $P(0)$ is a reference signal power at the input of the line, and $P(z)$ is the corresponding power at coordinate z. In the numerical computations in this paper we will always take $P(0)$ as the peak power. The modulated input field $M(t)$ is passed into a pre-compensating fiber, so that the field at the input of the line is $\tilde{A}(0,\omega) = \tilde{M}(\omega)\mathrm{e}^{j\frac{\omega^2}{2}\xi_{\mathrm{pre}}}$, where $\xi_{\mathrm{pre}} \triangleq -\ell_{\mathrm{pre}}\beta_{2,\mathrm{pre}}R^2$ is the normalized cumulated dispersion in the pre-compensation fiber of dispersion coefficient $\beta_{2,\mathrm{pre}}$ and length ℓ_{pre}. Now make the change of variable, [14]:

$$\tilde{A}(z,\omega) = \sqrt{P(0)}e^{\frac{\ln G(z) + jC(z)\omega^2}{2}}\tilde{U}(z,\omega)$$

where $C(z) \triangleq \xi_{\mathrm{pre}} + \xi_{\mathrm{in}}(z)$ is the total normalized cumulated dispersion up to z, where $\xi_{\mathrm{in}}(z) \triangleq -R^2\int_0^z \beta_2(s)\,\mathrm{d}s$ is the normalized cumulated dispersion along the line (i.e. the *in-line dispersion*). Differentiating and plugging in (1) one gets the nonperiodic DM-NLSE for general DM systems as:

$$\frac{\partial \tilde{U}(z,\omega)}{\partial z} = -j\Phi_{\mathrm{NL}} \iint_{-\infty}^{\infty} \frac{\gamma(z)G(z)\mathrm{e}^{-jC(z)\omega_1\omega_2}}{L\langle\gamma G\rangle}\tilde{U}(z,\omega+\omega_1)\tilde{U}(z,\omega+\omega_2)\tilde{U}^*(z,\omega+\omega_1+\omega_2)\frac{\mathrm{d}\omega_1}{2\pi}\frac{\mathrm{d}\omega_2}{2\pi} \tag{2}$$

where the nonlinear phase is defined as $\Phi_{\mathrm{NL}} \triangleq P(0)L\langle\gamma G\rangle$.

3. Regular and logarithmic perturbations

Treating $\Phi_{\rm NL}$ as a small parameter in (2), the first-order regular perturbation (RP1) solution of (2) on the link $[0, L]$ is (see e.g. [26]): $\tilde{U}(L,\omega) = \tilde{U}_0(\omega) - j\Phi_{\rm NL}\tilde{U}_1(L,\omega)$, where $\tilde{U}_0(\omega) \equiv \tilde{U}(0,\omega) = \tilde{M}(\omega)/\sqrt{P(0)}$ is the initial condition, the perturbative term is

$$\tilde{U}_1(L,\omega) \triangleq \iint_{-\infty}^{\infty} \tilde{\eta}(\omega_1\omega_2)\tilde{U}_0(\omega+\omega_1)\tilde{U}_0(\omega+\omega_2)\tilde{U}_0^*(\omega+\omega_1+\omega_2)\frac{\mathrm{d}\omega_1}{2\pi}\frac{\mathrm{d}\omega_2}{2\pi} \tag{3}$$

and the *DM kernel* is defined as

$$\tilde{\eta}(w) \triangleq \frac{\int_0^L \gamma(s)G(s)\mathrm{e}^{-jC(s)w}\mathrm{d}s}{\int_0^L \gamma(s)G(s)\mathrm{d}s} = \frac{\langle \gamma G\mathrm{e}^{-jCw}\rangle}{\langle \gamma G\rangle} \tag{4}$$

When $\gamma(z)$ is constant with z, the kernel simplifies to that given by Wei [14]. If in (4) one uses the difference $\Delta C = -R^2\int_0^z \Delta\beta_2(s)\,\mathrm{d}s$ with respect to the link average value instead of C, one gets the Ablowitz kernel for periodic systems [15].

For example, for a single uncompensated span with transmission fiber nonlinear coefficient γ, loss α, dispersion coefficient β_2, and "long" length $z_A \gg \frac{1}{\alpha}$, from (4) one gets: $\tilde{\eta}_1(w) = \frac{1}{1+j\mathcal{S}_T w}$, having defined the strength as, [3,5], $\mathcal{S}_T \triangleq -\frac{\beta_2}{\alpha}R^2$, which represents the accumulated dispersion over the span effective length $\frac{1}{\alpha}$. If instead the link is composed of N identical "long" spans, with transmission fiber parameters as above, with lumped amplification at the span end that recovers the span losses, with in-line dispersion per span $\xi_s \equiv \frac{\xi_{\rm in}}{N}$ and pre-compensation $\xi_{\rm pre}$, then from (4) one easily gets

$$\tilde{\eta}(w) = \mathrm{e}^{-j\xi_{\rm pre}w}\left[\frac{1}{N}\sum_{k=0}^{N-1}\mathrm{e}^{-j\xi_s k w}\right]\tilde{\eta}_1(w) = \mathrm{e}^{-j(\xi_{\rm pre}+\frac{N-1}{2}\xi_s)w}\left[\frac{1}{N}\frac{\sin(\frac{N\xi_s}{2}w)}{\sin(\frac{\xi_s}{2}w)}\right]\tilde{\eta}_1(w) \tag{5}$$

If one adds at the receiver a post-compensating fiber with cumulated normalized dispersion $\xi_{\rm post}$, one finally gets the RP1 approximate field at the receiver in the time domain as $A^{\rm RP1}(L,t) = A_0(L,t) - j\Phi_{\rm NL}A_1(L,t)$, where $\tilde{A}_0(L,\omega) = \sqrt{P(L)}\mathrm{e}^{j\frac{\xi_{\rm tot}\omega^2}{2}}\tilde{U}_0(\omega)$ is the linear term, and $\tilde{A}_1(L,\omega) = \sqrt{P(L)}\mathrm{e}^{j\frac{\xi_{\rm tot}\omega^2}{2}}\tilde{U}_1(L,\omega)$ the RP1 term, and we introduced the total (or *residual*) dispersion $\xi_{\rm tot} \triangleq C(L) + \xi_{\rm post} = \xi_{\rm pre} + \xi_{\rm in} + \xi_{\rm post}$, where for brevity we write $\xi_{\rm in}(L) \equiv \xi_{\rm in}$. Being the first term of a polynomial expansion in the *small* parameter $\Phi_{\rm NL}$, the RP1 solution is valid at small nonlinear phases, and has thus a serious energy-divergence problem at practical values of $\Phi_{\rm NL}$. A better fit with the actual output field at practical nonlinear phases is provided by the first-order logarithmic perturbation (LP1) [19,20,27]:

$$A^{\rm LP1}(L,t) = A_0(L,t)\exp\left\{-j\Phi_{\rm NL}\frac{A_1(L,t)}{A_0(L,t)}\right\} \tag{6}$$

which is calculated from the same first two terms of the RP solution.

We next present some numerical results to give an idea of the precision of the RP1/LP1 approximations. To facilitate interpretation of all numerical results, Appendix A summarizes the conversions from dimensionless to physical units.

3.1. Numerical checks on LP1, RP1 for single on-off keying channel

We considered an $N = 20$ span DM link with 100 km spans, with in-line linear dispersion compensation at each span end, full in line compensation ($\xi_{\rm in} = 0$), without pre and post-compensation. No optical/electrical filtering was applied at the receiver. A single non-return to zero (NRZ) on-off keying (OOK) channel was transmitted with raised-cosine supporting pulses in power with rolloff 0.4 and extinction ratio of 20 dB. Fig. 1 shows the received normalized power vs. normalized time, for both RP1/LP1 theory and split-step Fourier method (SSFM) simulation [25] calculated with 32 samples per bit and representing the true result. In Fig. 1, the top row shows the case of $R = 10$ Gb/s, with a practical phase of $\Phi_{\rm NL} = 0.6\pi$, while the bottom row the case of $R = 40$ Gb/s, and a smaller phase $\Phi_{\rm NL} = 0.3\pi$ (since the tolerable nonlinear phase decreases with bit rate). Transmission fiber was large effective area (LEAF$^{\rm TM}$)

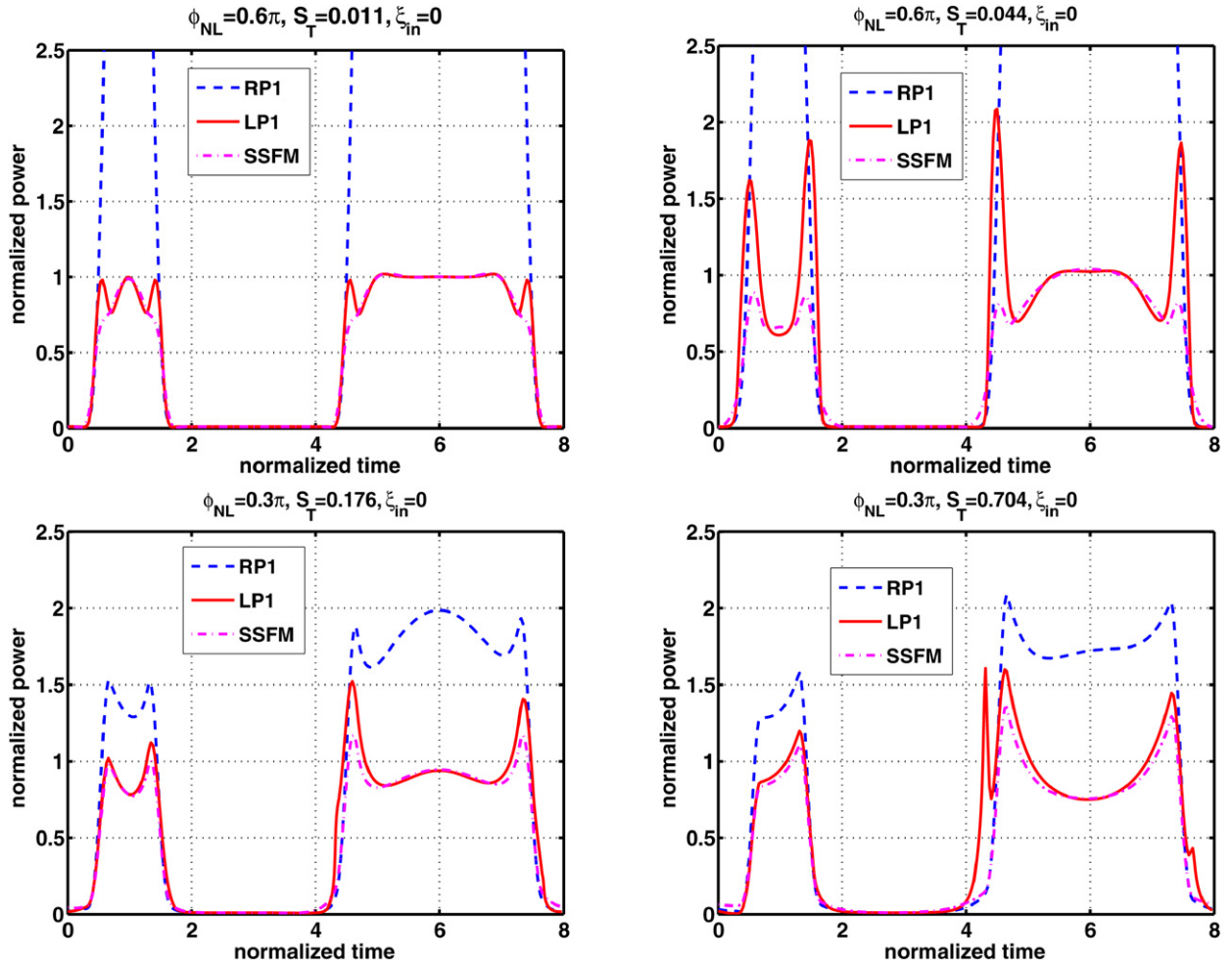

Fig. 1. Received Power vs. time for RP1 (dash), LP1 (solid), SSFM (dash-dot). DM system: 20×100 km OOK, $\xi_{\text{in}} = \xi_{\text{pre}} = \xi_{\text{post}} = 0$. Ext. ratio 20 dB. Left column: leaf fiber. Right column: SMF fiber. Top row: $R = 10$ Gb/s, $\Phi_{\text{NL}} = 0.6\pi$; Bottom row: $R = 40$ Gb/s, $\Phi_{\text{NL}} = 0.3\pi$.

($D_T = 4$ ps/nm/km) in the left column, and standard single mode (SMF) ($D_T = 16$ ps/nm/km) in the right column. We first note the power divergence of the RP1 method for larger nonlinear phases. We then note that LP1 is much closer to the true SSFM results, but tends to over-emphasize the pulse high frequencies, especially at larger nonlinear phases. In the $R = 40$ Gb/s case we also note that at the larger strengths ($\times 16$) implied by a $\times 4$ increase in bit rate also the LP1 approximation starts to have energy divergence problems with sharp spikes, which however occur when the RP1 solution is well behaved. Hence a modified LP1 solution, robust even at 40 Gb/s, can be devised as: $A^{\text{LP1,mod}}(L,t) = \min\{A^{\text{LP1}}(L,t), A^{\text{RP1}}(L,t)\}$ in order to remove such sharp spikes. Results similar to ours for LP1 at 10 Gb/s were obtained in a 5×100 km NRZ-OOK terrestrial link by Forestieri et al. [20,19]. Their LP1 was obtained by 5 cycles of the LP algorithm, where the LP1 field out of one span was the input to the next span. The good news is that our LP1 reproduces the output pulses with similar accuracy, but in a single computation of the LP1 kernel, instead of the repetition to which both the RP1 method used in [26] and Forestieri's LP1 are forced.

Finally, note that the computational complexity of a direct calculation of the RP1 double-integral (3) scales as the square of the number of time/frequency samples N_{FFT} in the Fast-Fourier transform window, instead of the $N_{\text{FFT}} \log N_{\text{FFT}}$ complexity of the SSFM approach. Hence the RP1/LP1 is mostly a tool of theoretical value, as we will show in the following sections. However, it was shown in [19] that the complexity of the LP1 method can be made comparable to that of the SSFM, while higher order LP approximations can be even more efficient than SSFM in the weakly nonlinear regime.

4. Time-domain analysis: kernel inversion

Wei [14] states that most of the time-domain treatments of quasi-linear DM systems [22] leading to the analysis of intersymbol interference, represented by inter-pulse cross-phase modulation (I-XPM) and inter-pulse four wave mixing (I-FWM), are based on the time-domain version of the RP1 solution with zero total dispersion: $A^{\mathrm{RP1}}(L,t) = \sqrt{P(L)}[U_0(t) - j\Phi_{\mathrm{NL}}U_1(L,t)]$, where the inverse Fourier transform of $\tilde{U}_1(L,\omega)$ in (3) is [15]:

$$U_1(L,t) = \iint_{-\infty}^{\infty} \eta(t_1 t_2) U_0(t+t_1) U_0(t+t_2) U_0^*(t+t_1+t_2)\,\mathrm{d}t_1\,\mathrm{d}t_2 \tag{7}$$

where $\eta(t_1t_2)$ is the inverse 2-D Fourier transform of $\tilde{\eta}(\omega_1\omega_2)$. From (4) we see that the DM kernel $\tilde{\eta}(w)$ is a function of the single variable $w \equiv \omega_1\omega_2$. For this class of 2-D Fourier transforms, the 2-D inverse transform is a function of the product $\tau = t_1t_2$, and can be obtained by first computing the 1-D inverse

$$J(c) = \int_{-\infty}^{\infty} \tilde{\eta}(w)\mathrm{e}^{+jwc}\frac{\mathrm{d}w}{2\pi}$$

with respect to variable w, and then the 2-D inverse transform is computed as [14]:

$$\eta(\tau) = \int_0^{\infty} \frac{J(\tau/y)\mathrm{e}^{jy} + J(-\tau/y)\mathrm{e}^{-jy}}{y}\,\frac{\mathrm{d}y}{2\pi} \tag{8}$$

From such a form, we find the following properties, valid for any kernel, that will be exploited later:

(i) $\eta(0) = -\frac{J(0)}{\pi}\,\mathrm{Ci}(0) = +\infty$, where $\mathrm{Ci}(x)$ is the cosine integral;

(ii) Let $J_e(c) = \frac{J(c)+J(-c)}{2}$ and $J_o(c) = \frac{J(c)-J(-c)}{2}$ be the even and odd parts of $J(c)$, respectively. Then

$$\eta(\tau) = \frac{2}{2\pi}\left[\int_0^{\infty} J_e\left(\frac{\tau}{y}\right)\frac{\cos y}{y}\,\mathrm{d}y + j\int_0^{\infty} J_o\left(\frac{\tau}{y}\right)\frac{\sin y}{y}\,\mathrm{d}y\right]$$

The major contribution of Wei [14] to the theory of DM comes from the physical interpretation he gave of the inverse transform $J(c)$ of $\tilde{\eta}(w)$: the variable $c \equiv C(z)$ is in fact the normalized cumulated dispersion along the line, and $J(c)$ can be shown to be a nonnegative function proportional to the power along the line, hence its name "Power Weighted Dispersion Distribution" (PWDD) [14]. Wei rightly gives great emphasis to the PWDD as a powerful intuitive tool for DM system optimization. Such a power in DM system optimization was already understood by Minzioni et al. [28], although not analytically justified in its full generality. Also, concepts similar to the PWDD had been previously used to establish the analytical models that lead to the well-known pre-compensation optimization rule [8,6].

We note here that $J(c)$ integrates to 1, since by definition $\tilde{\eta}(0) = 1$ for any map. Hence in probability theory parlance $J(c)$ is a probability density function (PDF) associated with a random variable (RV) C, and thus

$$\tilde{\eta}(-w) = \int_{-\infty}^{\infty} J(c)\mathrm{e}^{-j(-w)c}\,\mathrm{d}c = \mathbb{E}\big[\mathrm{e}^{jwC}\big]$$

is its characteristic function (CF). It is related to the moments of the RV C by the moment theorem [30]:

$$\tilde{\eta}(w) = \mathbb{E}\big[\mathrm{e}^{-jwC}\big] = \sum_{k=0}^{\infty}\frac{\mathbb{E}[C^k]}{k!}(-jw)^k \tag{9}$$

and conversely one gets the k-th moment of C as:

$$\mathbb{E}\big[C^k\big] = j^k\left.\frac{\mathrm{d}^k\tilde{\eta}(w)}{\mathrm{d}w^k}\right|_{w=0}$$

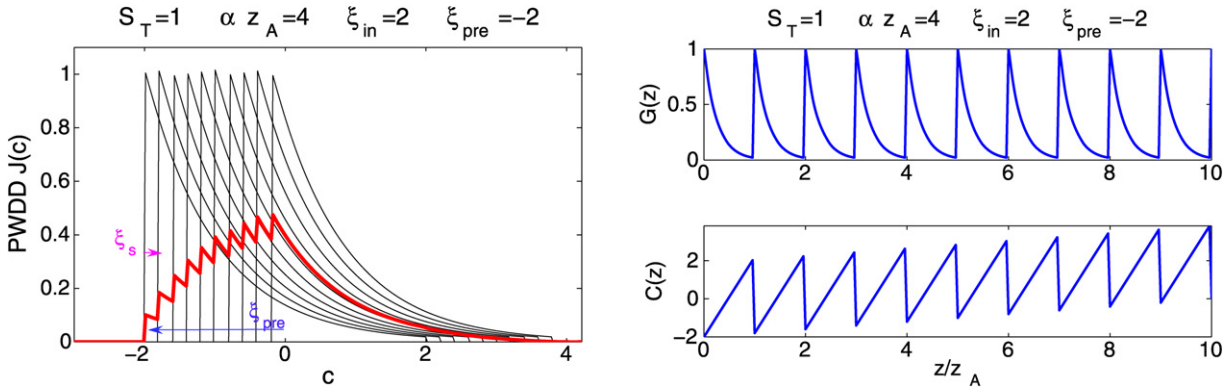

Fig. 2. (Left) Power-weighted dispersion distribution $J(c)$ for a DM link with strength $\mathcal{S}_T = 1$, span length $z_A = \frac{4}{\alpha}$, $\xi_{\text{pre}} = -2$; $\xi_{\text{in}} = 2$; (Right) Corresponding power gain $G(z)$ and normalized cumulated dispersion $C(z)$ versus z/z_A.

Let us now consider some examples of PWDD. For a single uncompensated span of length $z_A \gg \frac{1}{\alpha}$, with transmission fiber nonlinear coefficient γ, loss α and dispersion coefficient β_2 we already know the DM kernel $\tilde{\eta}_1(w)$, whose inverse transform is $J_1(c) = \frac{1}{|\mathcal{S}_T|} e^{-\frac{c}{\mathcal{S}_T}} U(c \cdot \text{sgn}(\mathcal{S}_T))$, where the unit step function is defined as $U(t)$=1 if $t \geqslant 0$, and zero otherwise. Its support is over positive c for $\mathcal{S}_T > 0$ and over negative c otherwise. $J_1(c)$ is the PDF of an exponential RV C_1 with average $\mathbb{E}[C_1] = \mathcal{S}_T$.

In the case of a link composed of N identical spans of length z_A, with same fiber parameters as above, the DM kernel was derived in (5). Inversion provides the system PWDD as

$$J(c) = \frac{1}{N} \sum_{k=1}^{N} J_1\big(c - \big[\xi_{\text{pre}} + (k-1)\xi_s\big]\big) \tag{10}$$

i.e., as the average of the PWDD of each span k, which is the uncompensated PWDD $J_1(c)$ shifted by the accumulated dispersion up to its beginning, namely $\xi_{\text{pre}} + (k-1)\xi_s$. Eq. (10) is an expression of the law of total probability: the RV C is obtained by choosing "at random" (i.e. equally likely) one of N spans, and then selecting the cumulated dispersion as a RV $C_k = C_1 + [\xi_{\text{pre}} + (k-1)\xi_s]$, where RV C_1 has PDF $J_1(c)$.

Fig. 2 (left) shows $J(c)$ (thick line) for a DM link composed of $N = 10$ spans, with strength $\mathcal{S}_T = 1$, span length $z_A = \frac{4}{\alpha}$, $\xi_{\text{pre}} = -2$; $\xi_{\text{in}} = 2$, while Fig. 2 (right) shows the corresponding gain $G(z)$ and "dispersion map" $C(z)$ versus normalized distance z/z_A. In Fig. 2 (left) we also report in thin line the constituent PDFs $J_k(c) \equiv J_1(c - [\xi_{\text{pre}} + (k-1)\xi_s])$ in Eq. (10) for all $k = 1, \ldots, N$, where the shift due to pre-compensation ξ_{pre} and in-line compensation per span ξ_s are shown by arrows. By applying the total probability law we easily get the average as: $\mathbb{E}[C] = \xi_{\text{pre}} + \mathcal{S}_T + \frac{N-1}{2}\xi_s$.

4.1. Optimal DM

Wei claims that *optimal DM sets to zero the median of the RV C associated with the PWDD J(c) of the link* ([14], p. 2545). It is known instead that the best choice for weakly nonlinear systems is to let $\text{Im}(\tilde{\eta}(w)) = 0$ [31]. In the framework of this article, the proof is now simple: $\text{Im}(\tilde{\eta}(w)) = 0$ implies by the moment theorem (9) that all *odd* moments $\mathbb{E}[C^k]$, $k = 1, 3, 5, \ldots$, of the RV C are zero. A necessary and sufficient condition for this to happen is that $J(c)$ is *even*: such a $J(c)$ corresponds to a so called *symmetric map*. From property (ii) of (8) we know that an *even* $J(c)$ corresponds to a *real* kernel impulse response $\eta(t_1 t_2)$, and thus to a purely imaginary nonlinear distortion when the input field $U_0(t)$ is real, as per Eq. (7): the intensity of the field is thus preserved. This concludes the proof.

With long lossy spans made of a single kind of transmission fiber, the overall $J(c)$ cannot be symmetric. When using a pre-compensation fiber to ameliorate link performance, all that one can do is to shift $J(c)$ by an amount ξ_{pre} so as to minimize $|\text{Im}(\tilde{\eta}(w))|$ as much as possible. Since odd moments are typically arranged in decreasing order ($|\mathbb{E}[C]| \gg |\mathbb{E}[C^3]| \gg |\mathbb{E}[C^5]| \gg \cdots$), then the best that one can do with a pre-fiber is to zero out the largest odd moment: $\mathbb{E}[C] = 0$. This is what we call the "straight-line rule" (SLR) for setting the optimal pre-compensation [31,6–8]. For instance, in the identical N lossy span case, this leads to the choice $\xi_{\text{pre}} = -\mathcal{S}_T - \frac{N-1}{2}\xi_s$, which in dimensional

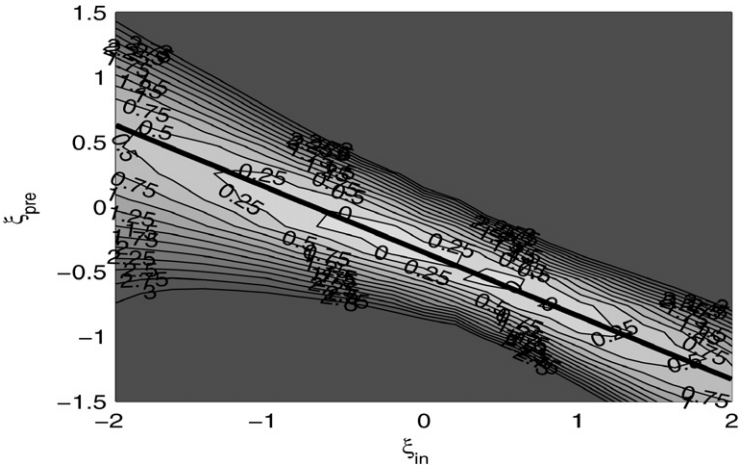

Fig. 3. SSFM-simulated contours of OSNR penalty [dB] @BER $= 10^{-5}$ vs. $\xi_{\rm pre}$ and $\xi_{\rm in}$, with optimized $\xi_{\rm post}$. NRZ-OOK link with 20×100 km, $D_T = 8$ ps/nm/km, $R = 40$ Gb/s (i.e. $\mathcal{S}_T = 0.35$), and $\Phi_{\rm NL} = 0.15\pi$. Solid straight line: SLR.

units translates as: $D_{\rm pre} = -\frac{D_T}{\alpha} - \frac{N-1}{2} D_s$ [ps/nm], where D_T [ps/nm/km] is the dispersion of the transmission fiber, and D_s [ps/nm] the per-span in-line dispersion. As an example, Fig. 3 shows contours of the penalty [dB] on optical signal to noise ratio (OSNR) at bit error rate BER $= 10^{-5}$ versus in-line $\xi_{\rm in}$ and pre-compensation $\xi_{\rm pre}$ for a 20×100 km 40 Gb/s NRZ-OOK link with Teralight$^{\rm TM}$ fiber ($D_T = 8$ ps/nm/km). The analytical SLR is shown to closely follow the locus of lowest penalty.

5. LP1 response to Gaussian pulse and optimal post-compensation

We now derive a new "optimal" rule for choosing the post-compensation dispersion. To this aim, we investigate the response of a DM system to a single Gaussian pulse, with peak power-normalized form

$$U_0(t) = \mathrm{e}^{-t^2/(2T_0^2)}$$

where $T_0 = d/2$ is the half-width. Our idea is to exploit the excellent LP1 approximation (6) in the case $\xi_{\rm tot} = 0$, and further approximate it by a first-order Taylor expansion in t of the argument of the exponential as:

$$A^{\rm LP1}(L,t) \cong \mathrm{e}^{-j\Phi_{\rm NL}U_1(0)} \sqrt{P(L)}\, U_0(t) \mathrm{e}^{\{-j\Phi_{\rm NL}[U_1^{(2)}(0)/2 + \frac{2}{d^2}U_1(0)]t^2\}}$$

where in brief we write $U_1(L,t) \equiv U_1(t)$, and $U^{(2)}(0)$ is the second derivative of $U_1(t)$ at $t = 0$. The rationale is that the output pulse looks now like a chirped Gaussian pulse, so that the search for the appropriate extra post-compensating fiber to be added to the $\xi_{\rm tot} = 0$ system to optimally compress the received pulses and improve performance is made analytically feasible. Define the complex parameter $a \equiv a_R + j a_I \triangleq -U_1(0) - \frac{d^2}{4} U_1^{(2)}(0)$. Then one gets

$$A^{\rm LP1}(L,t) \cong \mathrm{e}^{-j\Phi_{\rm NL}U_1(0)} \sqrt{P(L)} \mathrm{e}^{-[1-j2\Phi_{\rm NL}b]2t^2/d_{\rm eq}^2} \tag{11}$$

where we defined

$$b \triangleq \frac{a_R}{2(1+\Phi_{\rm NL}a_I)}, \qquad d_{\rm eq} \triangleq \frac{d}{\sqrt{1+\Phi_{\rm NL}a_I}} \tag{12}$$

assuming $1 + \Phi_{\rm NL}a_I > 0$. For pure SPM (i.e. when the strength $\mathcal{S}_T \to 0$) we have that $U_1(t) = |U_0(t)|^2 U_0(t)$, hence $a = 2$, and thus $b = 1$ and $d_{\rm eq} = d$. With such definitions, we note that, apart for an irrelevant multiplying factor, the output pulse is approximately still Gaussian with duty cycle $d_{\rm eq}$ and linear chirp parameter $c \equiv 2\Phi_{\rm NL}b$. The values of U_1 needed in the calculation of b and $d_{\rm eq}$ can be evaluated as

$$U_1(0) = \int_{-\infty}^{\infty} \tilde{U}_1(\omega) \frac{\mathrm{d}\omega}{2\pi}, \qquad \text{and} \qquad U_1^{(2)}(0) = -\int_{-\infty}^{\infty} \omega^2 \tilde{U}_1(\omega) \frac{\mathrm{d}\omega}{2\pi}$$

Calculations do have a simple form if we approximate $\tilde{\eta}_1(w) = \frac{1}{1+j\mathcal{S}_T w} \cong \mathrm{e}^{-j\mathcal{S}_T w}$, an approximation valid over the signal frequency range when $\mathcal{S}_T \ll \frac{d^2}{8}$. With such an approximation the needed integrals can be computed in closed form, as shown in Appendix B:

$$U_1(0) \cong \frac{1}{N}\sum_{k=0}^{N-1} \frac{d^2}{\sqrt{48(\xi_{\mathrm{pre}}+\mathcal{S}_T+k\xi_s)^2+d^4+j8d^2(\xi_{\mathrm{pre}}+\mathcal{S}_T+k\xi_s)}}$$
$$U_1^{(2)}(0) \cong -\frac{1}{N}\sum_{k=0}^{N-1} \frac{4[3d^2+j4(\xi_{\mathrm{pre}}+\mathcal{S}_T+k\xi_s)]}{[d^2+j12(\xi_{\mathrm{pre}}+\mathcal{S}_T+k\xi_s)]\sqrt{48(\xi_{\mathrm{pre}}+\mathcal{S}_T+k\xi_s)^2+d^4+j8d^2(\xi_{\mathrm{pre}}+\mathcal{S}_T+k\xi_s)}} \tag{13}$$

Let us first check the numerical dependence of the b parameter in (12) on DM. First of all, let's note from (5) that the DM kernel can be approximated as

$$\tilde{\eta}(w) \cong \left[\frac{1}{N}\frac{\sin(\frac{\xi_{\mathrm{in}}}{2}w)}{\sin(\frac{\xi_{\mathrm{in}}}{2N}w)}\right]\mathrm{e}^{-j(\xi_{\mathrm{pre}}+\mathcal{S}_T+\frac{N-1}{2}\frac{\xi_{\mathrm{in}}}{N})w}$$

Thus when we choose the SLR optimal pre-compensation the exponential disappears and the DM kernel is real and *only depends on in-line* ξ_{in} *and not on strength*. The terms $U_1(0)$ and $U_1^{(2)}(0)$ are also purely real, and so is a, while $d_{\mathrm{eq}} = d$ and $b = a/2$, independent of Φ_{NL}. In such a *SLR-compensated case*, therefore, Eq. (11) reveals that things go (up to second order in a Taylor expansion of the phase) as if the *DM system were a pure SPM block*, with an effective nonlinear phase $\Phi_{\mathrm{NL}}^{\mathrm{eff}} = |b|\Phi_{\mathrm{NL}}$. We thus call b the *nonlinear phase factor*. Fig. 4 (left) shows b in (12) versus in-line ξ_{in} for various span numbers, for a DM system with SLR pre, $\xi_{\mathrm{tot}} = 0$ and Gaussian pulses with duty $d = 0.685$. Results are independent of nonlinear phase, and of strength as long as approximation $\frac{1}{1+j\mathcal{S}_T w} \cong \mathrm{e}^{-j\mathcal{S}_T w}$ holds. We note an alternating behavior with increasing N, even N values giving a smaller b than odd N values. We also note that b can become negative, implying an inversion of the sign of the nonlinear induced chirp with respect to that of pure SPM. The convergence for increasing N occurs starting at small ξ_{in} values, and extending to larger in-line as N increases. For large enough N the behavior is decreasing monotone. The message from such a result is very important: the effective nonlinear phase in a SLR pre-compensated DM periodic system tends to vanish for large in-line dispersion, independently of the strength. This is the essence of the so-called quasi-linear propagation regime [22]. Finally, for fixed finite ξ_{in}, let us take the limits of (13) for vanishing duty cycle: we get $\lim_{d\to 0} U_1(0) = 0$ and $\lim_{d\to 0} \frac{d^2}{4} U_1^{(2)}(0) = 0$. Hence $a \to 0$, and so does b. Thus, *low duty cycle pulses suffer less from nonlinear distortion*.

Let us now try to understand how close the above analytical results are to reality. Fig. 4 (center for $\xi_{\mathrm{in}} = 0.2$ and right for $\xi_{\mathrm{in}} = 0.8$) shows received phase (rad) vs. normalized time in a DM system with strength $\mathcal{S}_T = 0.022$ ($D = 8$ ps/nm/km at 10 Gb/s), $N = 50$ spans, nonlinear phase $\Phi_{\mathrm{NL}} = 0.3\pi$, SLR pre-compensation, and $\xi_{\mathrm{tot}} = 0$, when a Gaussian pulse with duty $d = 0.685$ is launched at time $t = 3$. SSFM simulations are shown in the dashed line, while the parabolic approximate phase in (11) is shown in the solid line, and it matches well the SSFM phase at the pulse center. The negative concavity in the right plot corresponds to a negative b.

Since the output pulses in the above zero total dispersion DM system are approximately chirped Gaussian, the value of the optimal extra post-compensation can now be derived from well known results on the optimal compression of chirped Gaussian pulses by pure GVD [32]. If we let β_2 and ℓ be the GVD and length of the extra post compensation with normalized cumulated dispersion $\xi_* = -\beta_2 \ell R^2$, then maximum pulse compression is obtained when, [32],

$$-\frac{\beta_2 \ell}{T_0^2} = \frac{c}{1+c^2}$$

i.e. when:

$$\frac{\xi_*}{(d_{\mathrm{eq}}/2)^2} = \frac{2\Phi_{\mathrm{NL}} b}{1+4\Phi_{\mathrm{NL}}^2 b^2}$$

so that the optimal overall total dispersion $\xi_{\mathrm{tot}} \equiv 0 + \xi_*$ is

$$\xi_{\mathrm{tot}} = \frac{d_{\mathrm{eq}}^2}{2}\frac{\Phi_{\mathrm{NL}} b}{1+4\Phi_{\mathrm{NL}}^2 b^2} \tag{14}$$

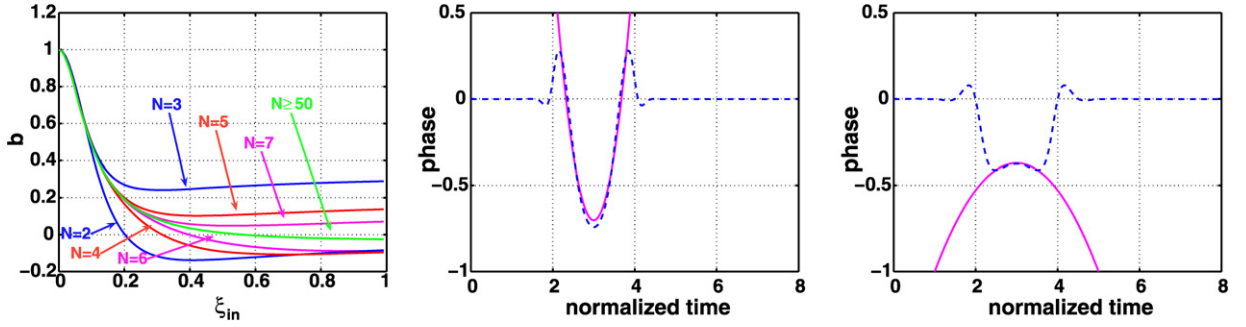

Fig. 4. (Left): Nonlinear phase factor b versus in-line ξ_{in} for various spans N, for a DM system with SLR pre, $\xi_{\text{tot}} = 0$ and Gaussian pulses with duty $d = 0.685$. (Center + right): Received field phase (rad) vs. time for Gaussian input with duty $d = 0.685$ and 30 dB of extinction ratio. Solid: theory (11); dashed: SSFM simulation. DM system data: $N = 50$ spans, $\mathcal{S}_T = 0.022$, SLR pre, $\xi_{\text{tot}} = 0$, $\Phi_{\text{NL}} = 0.3\pi$, $\xi_{\text{in}} = 0.2$ (center), $\xi_{\text{in}} = 0.8$ (right).

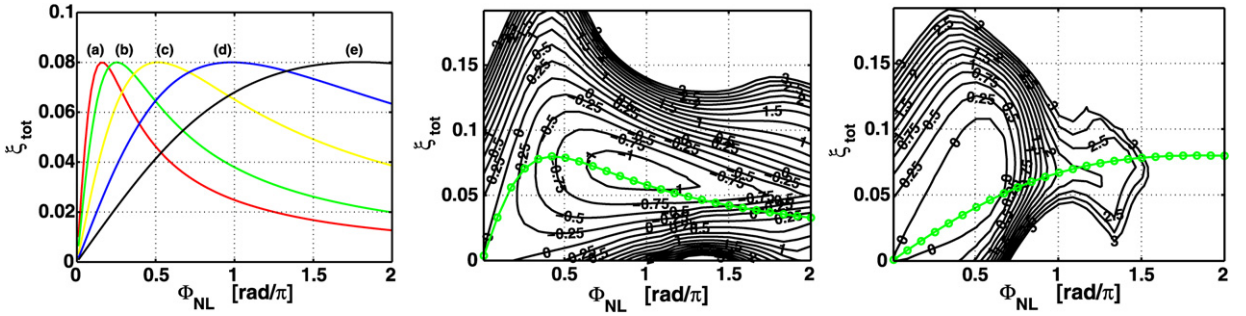

Fig. 5. (Left) Optimal ξ_{tot} (14) vs. nonlinear phase Φ_{NL} for several values of $\xi_{\text{in}} = 0$ (a), $\xi_{\text{in}} = 0.1$ (b), $\xi_{\text{in}} = 0.2$ (c), $\xi_{\text{in}} = 0.3$ (d), $\xi_{\text{in}} = 0.4$ (e), for a DM system with $N = 50$ spans, SLR pre, and Gaussian pulses $d = 0.8$; (Center) SP [dB] contours vs. ξ_{tot} and Φ_{NL} for $\xi_{\text{in}} = 0.17$ and optimal ξ_{tot} vs. Φ_{NL} (14) (circles); (Right) SP [dB] contours for $\xi_{\text{in}} = 0.40$ and optimal ξ_{tot} (14) (circles).

Fig. 5 (left) shows the optimal ξ_{tot} (14) vs. nonlinear phase Φ_{NL} for several values of $\xi_{\text{in}} = 0$, 0.1, 0.2, 0.3, 0.4 for a DM system with $N = 50$ spans, SLR pre-compensation, $\xi_{\text{tot}} = 0$ and Gaussian pulses with duty $d = 0.8$. Such curves are all Φ_{NL}-scaled versions of the $\xi_{\text{in}} = 0$ curve. Fig. 5 (center) shows instead for the same DM line with $\xi_{\text{in}} = 0.17$ (simulated with $D_T = 8$ ps/nm/km at $R = 10$ Gb/s, i.e. $\mathcal{S}_T = 0.022$) the "true" system performance for OOK modulation, obtained as SSFM-simulated contours of the sensitivity penalty (SP) in decibels at a BER $= 10^{-5}$ versus ξ_{tot} and Φ_{NL}. Fig. 5 (right) shows the same plot for a system with a larger in-line $\xi_{\text{in}} = 0.40$. The superposed curves with circles represent the best ξ_{tot} from theory (14), and a reasonable qualitative match with the lowest penalty contour is observed in both plots (note that at $\xi_{\text{in}} = 0.40$ the penalty diverges at much lower nonlinear phases).

6. Inter-pulse interactions

In the previous section we have seen that a single pulse gets less and less distortion from the DM line as its in-line dispersion ξ_{in} increases. It is known that single-pulse distortions decrease also when the strength is increased [15]. However, a large ξ_{in} or a large $\mathcal{S}_T$ give large inter-pulse interactions, hence an increased inter-symbol interference, as we show next.

Assume the input signal is a pulse amplitude modulation: $U_0(t) = \sum_{k=-\infty}^{\infty} b_k\, p(t-k)$, where $p(t)$ is the supporting pulse with normalized duration (or duty cycle) d, and b_k the modulating symbol at the k-th symbol interval. The supporting pulse field is return-to-zero (RZ), i.e., $p(t) = p(0)$ for $|t| \leqslant d/2$ and zero otherwise, where $p(0)$ is the peak power. Substituting in (7) one gets, [14],

$$U_1(L,t) = \sum_{m=-\infty}^{\infty} \sum_{n=-\infty}^{\infty} \sum_{l=-\infty}^{\infty} b_m b_n b_l^* \iint_{-\infty}^{\infty} \eta(t_1 t_2)\, p(t+t_1-m)\, p(t+t_2-n)\, p(t+t_1+t_2-l)\, \mathrm{d}t_1\, \mathrm{d}t_2 \qquad (15)$$

To find the symbol indexes (m,n,l) that contribute nonzero terms on the reference symbol interval centered at $t_0 = 0$ it is easiest to assume [16] that $p(t) \cong dp(0)\delta(t)$, i.e., the supporting pulses have a very small duty cycle and thus look like delta functions with respect to the time DM kernel. The double integral in (15) becomes $\eta((t-m)(t-n))\delta(t-(m+n-l))$, so that the only slots that contribute are those satisfying the "time-matching" condition $m+n-l = t_0 \equiv 0$. Thus for very low duty cycle pulses the RP1 solution with zero total dispersion drastically simplifies to: $A^{\mathrm{RP1}}(L,t) = \sqrt{P(L)}[b_0 p(t) - j\Phi_{\mathrm{NL}} U_1(L.t)]$, with, [14],

$$U_1(L,t) = p(t)\cdot d^2 p(0)^2 \sum_{m,n,l} b_m b_n b_l^* \eta\big((m-l)(n-l)\big) \tag{16}$$

for all $|t| < 1/2$ in the zero-th slot, whose information symbol is b_0. Note that, since from property (i) of (8) it is $\eta(0) = +\infty$ for any kernel, then the self-phase modulation (SPM) term ($m = n = l$) and IXPM terms ($m = l$ or $n = l$) are incorrectly treated since the corresponding terms in (16) diverge. Hence the perturbation included in (16) is only that due to IFWM. The energy shed by IFWM on spaces ($b_0 = 0$) generates the so-called *ghost-pulses*, while on marks ($b_0 = 1$) it gives rise to the so-called *amplitude jitter* [16]. It can be shown that, in these $\xi_{\mathrm{tot}} = 0$ systems, IXPM instead gives rise to a purely imaginary (i.e. phase) distortion and thus does not contribute to amplitude jitter [16]. We will next show how IFWM induced distortions evolve with both in-line dispersion and map strength.

To this purpose, we consider a single channel OOK transmission with a special modulation pattern, where N_R consecutive interfering marks ($b_m = 1$, $1 \leqslant m \leqslant N_R$) follow the symbol of interest b_0 (we call them post-cursors), while all remaining symbols are spaces ($b_m = 0$) [21]. At the center $t = 0$ of the reference symbol, both the "ghost-pulse" field on a space ($b_0 = 0$) and the field variation on a mark ($b_0 = 1$) can be seen from (16) to be proportional to the following summation extended to all nonzero indexes m,n,l with $m \neq l$ and $n \neq l$ such that $b_m = b_n = b_l = 1$:

$$S(N_R) \triangleq \sum_{m,n,l} \eta\big((m-l)(n-l)\big) = \sum_{p=1}^{\lfloor N_R/2 \rfloor} \eta\big(p^2\big) + 2\sum_{p=1}^{\lfloor N_R/2 \rfloor} \sum_{q=p+1}^{N_R-p} \eta(pq)$$

where on the right we have the explicit computation, with $p = n-l$, $q = m-l$. One can thus define the following two quantities to characterize the impact of IFWM on spaces and marks: (i) the normalized ghost-pulse intensity

$$I_G(N_R) \triangleq \left|\frac{U_1(L,0)}{d^2 p(0)^3}\right|^2 = \big|S(N_R)\big|^2$$

and (ii) the normalized Mark relative intensity distortion (RID)

$$\Delta I_M(N_R) \triangleq \mathrm{Im}\left[\frac{U_1(L,0)}{d^2 p(0)^3}\right] = \mathrm{Im}\big[S(N_R)\big]$$

Fig. 6 shows both $I_G(N_R)$ (left) and $\Delta I_M(N_R)$ (center) versus the number of consecutive mark post-cursors N_R for a $N = 10$ span DM system with lossless spans of $z_A = 50$ km each, whose explicit time kernel expression, using (10), is

$$\eta(\tau) = \frac{1}{2\pi|C_T|}\frac{1}{N}\sum_{k=1}^{N}\left[E_1\left(-j\frac{\tau}{C_T + \xi_{\mathrm{pre}} + (k-1)\xi_s}\right) + E_1\left(-j\frac{\tau}{\xi_{\mathrm{pre}} + (k-1)\xi_s}\right)\right] \tag{17}$$

with $E_1(x)$ the exponential integral, and $C_T = -\beta_2 z_A R^2$ the dispersion cumulated over each span, which plays in this lossless case the role of the span strength.

The values for three maps are shown: 1) a map without in-line compensation and no pre-compensation [29]; 2) a map without in-line compensation and optimal SLR pre-compensation $\xi_{\mathrm{pre}} = -NC_T/2$ [29], and 3) a map with in-line dispersion $\xi_{\mathrm{in}} = 0.1C_T$ and optimal SLR pre-compensation $\xi_{\mathrm{pre}} = -C_T - \frac{N-1}{2}\xi_s$. For map 1 we note large values of both ghost pulse intensity and mark RID, with a long "memory", i.e. significant IFWM interference from post-cursors placed several hundred bit times away from the reference bit. In map 2 we chose the optimal SLR pre-compensation, which significantly decreases the ghost-pulse intensity even in the absence of in-line compensation, and completely suppresses the mark RID, since in the lossless case the PWDD is exactly symmetric. Finally in map 3 we note the dramatic reduction of ghost-pulse intensity with respect to the case without in-line, along with the complete suppression of mark RID with the SLR pre-compensation.

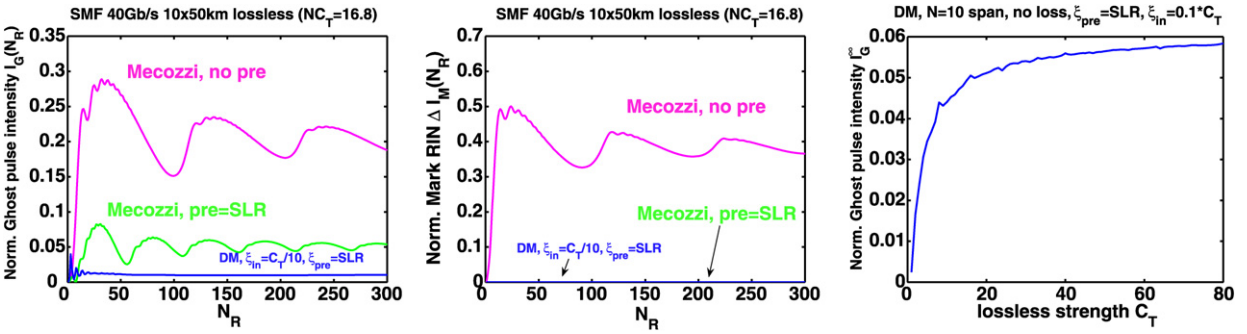

Fig. 6. (Left) ghost-pulse intensity I_G and (center) mark relative intensity distortion ΔI_M versus number of consecutive mark post-cursors N_R for a 10×50 km lossless link with total strength $NC_T = 16.8$ for the tree maps: 1) $\xi_{\text{in}} = 0$, $\xi_{\text{pre}} = 0$; 2) $\xi_{\text{in}} = 0$, $\xi_{\text{pre}} = SLR$; 3) $\xi_{\text{in}} = 0.1C_T$, $\xi_{\text{pre}} = SLR$. (Right): Asymptotic norm. ghost pulse intensity I_G^{∞} versus span strength C_T. DM lossless system with $N = 10$ spans, SLR pre-compensation at $\xi_{\text{in}}/C_T = 0.1$.

Fig. 6 (right) shows the asymptotic "floor" $I_G^{\infty} = \lim_{N_R \to \infty} I_G(N_R)$ versus per-span strength C_T, in the DM case with SLR pre-compensation and in-line $\xi_{\text{in}}/C_T = 0.1$. We observe an almost monotonic increase with strength, with a converging behavior at $C_T \to \infty$. This implies that, even with in-line compensation, ghost-pulses increase with increasing strength, thus deteriorating performance. The limiting value can be found by noting that $\lim_{N_R \to \infty} S(N_R) = \sum_{p=1}^{\infty} \sum_{q=1}^{\infty} \eta(pq)$. When $|C_T| \to \infty$ the double summation becomes a double integral, since in that case $\eta(t_1 t_2)$ becomes infinitely spread in the time domain: $\lim_{|C_T| \to \infty} S(\infty) = \int_0^{\infty} \int_0^{\infty} \eta(t_1 t_2)\, \mathrm{d}t_1\, \mathrm{d}t_2$. Now, since $1 = \tilde{\eta}(0) = \iint_{-\infty}^{\infty} \eta(t_1 t_2)\, \mathrm{d}t_1\, \mathrm{d}t_2$ and $\eta(\tau)$ has Hermitian symmetry, then $\int_0^{\infty} \int_0^{\infty} \mathrm{Re}[\eta(t_1 t_2)]\, \mathrm{d}t_1\, \mathrm{d}t_2 = \frac{1}{4}$. Since the map is symmetric, then $\eta(\tau)$ is real and thus $\lim_{|C_T| \to \infty} S(\infty) = 1/4$. Hence the sought asymptotic value is $\lim_{|C_T| \to \infty} I_G^{\infty} = (\frac{1}{4})^2 \sim 0.0625$, as visible in Fig. 6 (right). Similar results for mark RID in a lossy DM system appeared in [16], however without any hint to the asymptotic value.

7. RP1 extension to WDM

When all fiber parameters are the same for all channels the RP1/LP1 single-channel approach simply extends to the WDM case with minimum channel spacing $\Delta\lambda$ as follows. Express the aggregate WDM signal envelope w.r.t. the reference frequency f_r as $U(z,t) = \sum_{s=-N_c}^{N_c} U_s(z,t) \mathrm{e}^{-js\Delta\omega t}$, where $\Delta\omega \triangleq \frac{2\pi}{\eta_S d} > 0$ is the normalized frequency spacing, and we defined the fractional bandwidth utilization as $\eta_S \triangleq \frac{R/d}{\Delta f}$ [bit/s/Hz], where the frequency spacing is $\Delta f = \frac{c}{\lambda_r^2} \Delta\lambda > 0$ and R/d is an estimate of the modulated signal bandwidth. Now plug the Fourier transform $\tilde{U}(z,\omega)$ into the RP1 solution expressed with respect to the retarded time frame of the reference channel $r = 0$, and single out the propagation equation for reference channel $r = 0$, which after a change of variables can be expressed as: $\tilde{U}_r(L,\omega) = \tilde{U}_{0r}(\omega) - j\Phi_{\text{NL}} \tilde{U}_{1r}(L,\omega)$, with an RP1 perturbation

$$\tilde{U}_{1r}(L,\omega) = \sum_{m,n,l} \iint_{-\infty}^{\infty} \eta\left[\left(\omega_1 + \frac{2\pi(n-l)}{\eta_S d}\right)\left(\omega_2 + \frac{2\pi(m-l)}{\eta_S d}\right)\right] \times \tilde{U}_{0m}(\omega+\omega_1)\tilde{U}_{0n}(\omega+\omega_2)\tilde{U}_{0l}^*(\omega+\omega_1+\omega_2)\frac{\mathrm{d}\omega_1}{2\pi}\frac{\mathrm{d}\omega_2}{2\pi} \tag{18}$$

which is the sum of SPM ($m = n = l = r$), XPM ($m = r \neq n = l$) and FWM in all remaining (m,n,l) cases such that $m + n - l = r$. The total LP1 field is then

$$A_r^{\text{LP1}}(L,t) = A_{0r}(L,t) \exp\left\{-j\Phi_{\text{NL}} \frac{A_{1r}(L,t)}{A_{0r}(L,t)}\right\}$$

with

$$\tilde{A}_{0r}(L,\omega) = \sqrt{P(L)} \mathrm{e}^{j\frac{\xi_{\text{tot}}\omega^2}{2}} \tilde{U}_r(0,\omega)$$

the linear term, and

$$\tilde{A}_{1r}(L,\omega) = \sqrt{P(L)}\mathrm{e}^{j\frac{\xi_{\mathrm{tot}}\omega^2}{2}}\tilde{U}_{1r}(L,\omega)$$

the RP1 term. It is possible to prove that all major classical results concerning FWM and XPM can be derived from the RP1 perturbation (18). As an illustration, we will next show how well-known results on XPM filtering [33,23,24] can be obtained and generalized.

7.1. XPM filters

Consider now the case of a continuous wave (CW) probe signal $U_{0r}(t) = 1$ on the reference channel, and a single, sinusoidally amplitude-modulated pump field $U_{0p}(t) = 1 + m\cos(\omega_m t)$ on channel $p \neq 0$, where $0 < m < 1$ is the modulation index, and ω_m the sinusoidal modulation pulsation. Plugging the input field Fourier transform into (18), and keeping only linear terms in m, we get in the time-domain:

$$U_{1r}^{\mathrm{XPM}}(L,t) = 2 + m\big[H_p(\omega_m)\mathrm{e}^{j\omega_m t} + H_p(-\omega_m)\mathrm{e}^{-j\omega_m t}\big]$$

where the term 2 accounts for the XPM due to the CW component, and we defined

$$H_p(\omega_m) \triangleq \left[\eta\left[\omega_m\left(\omega_m + p\frac{2\pi}{\eta_S d}\right)\right] + \eta\left[\omega_m p\frac{2\pi}{\eta_S d}\right]\right] \tag{19}$$

The LP1 solution is thus $A_r^{\mathrm{LP1}}(L,t) = \sqrt{P(L)}\exp\{-j\Phi_{\mathrm{NL}}(1 + U_{1r}^{\mathrm{XPM}}(L,t) \otimes h_{\xi_{\mathrm{tot}}}(t))\}$, where $h_{\xi_{\mathrm{tot}}}(t)$ is the impulse response of the pure GVD filter with cumulated dispersion ξ_{tot}, so that

$$U_{1r}^{\mathrm{XPM}}(L,t) \otimes h_{\xi_{\mathrm{tot}}}(t) = 2 + m\mathrm{e}^{j\frac{\xi_{\mathrm{tot}}\omega_m^2}{2}}\big[H_p(\omega_m)\mathrm{e}^{j\omega_m t} + H_p(-\omega_m)\mathrm{e}^{-j\omega_m t}\big] \tag{20}$$

The XPM-induced phase of the output LP1 field on probe channel r is thus the imaginary part of the XPM-induced argument of the exponential

$$\theta_r^{\mathrm{XPM}}(t) \triangleq -\Phi_{\mathrm{NL}}\,\mathrm{Re}\big[U_{1r}^{\mathrm{XPM}}(L,t) \otimes h_{\xi_{\mathrm{tot}}}(t)\big]$$

while the intensity normalized to its reference CW power level in absence of XPM is

$$\frac{I_r(L,t)}{P(L)} = \mathrm{e}^{2\Phi_{\mathrm{NL}}\,\mathrm{Im}[U_{1r}^{\mathrm{XPM}}(L,t)\otimes h_{\xi_{\mathrm{tot}}}(t)]}$$

hence the XPM-induced relative intensity distortion (RID) is

$$\Delta I_r^{\mathrm{XPM}}(t) \triangleq \frac{I_r(L,t)}{P(L)} - 1 = \mathrm{e}^{2\Phi_{\mathrm{NL}}\,\mathrm{Im}[U_{1r}^{\mathrm{XPM}}(L,t)\otimes h_{\xi_{\mathrm{tot}}}(t)]} - 1$$

As shown in Appendix C, retrieving the sinusoidal components at frequency ω_m of both phase and intensity (for intensity, assuming distortions are small), one can express both phase and intensity as filterings of the input pump power $P_{0p}(t) = |U_{0p}(t)|^2$:

$$\tilde{\theta}_r^{\mathrm{XPM}}(\omega) = \tilde{P}_{0p}(\omega)H_{\text{IM-PM},p}(\omega), \qquad \tilde{\Delta I}_r^{\mathrm{XPM}}(\omega) = \tilde{P}_{0p}(\omega)H_{\text{IM-IM},p}(\omega)$$

where

$$\begin{aligned} H_{\text{IM-PM},p}(\omega) &= -\frac{\Phi_{\mathrm{NL}}}{2}\big[\mathrm{e}^{j\frac{\xi_{\mathrm{tot}}\omega^2}{2}}H_p(\omega) + \mathrm{e}^{-j\frac{\xi_{\mathrm{tot}}\omega^2}{2}}H_p^*(-\omega)\big] \\ H_{\text{IM-IM},p}(\omega) &= -j\Phi_{\mathrm{NL}}\big[\mathrm{e}^{j\frac{\xi_{\mathrm{tot}}\omega^2}{2}}H_p(\omega) - \mathrm{e}^{-j\frac{\xi_{\mathrm{tot}}\omega^2}{2}}H_p^*(-\omega)\big] \end{aligned} \tag{21}$$

For instance, for a DM terrestrial link with N identical "long" spans with precompensation ξ_{pre}, in-line ξ_{in} and strength $\mathcal{S}_T = -\frac{\beta_2}{\alpha}R^2$, whose kernel is given in (5), denoting with $\Delta\omega \equiv \frac{2\pi}{\eta_S d}$ the normalized channel frequency spacing, we get from (19)

$$H_p(\omega) = \mathrm{e}^{-j(\xi_{\mathrm{pre}}+\frac{N-1}{2}\frac{\xi_{\mathrm{in}}}{N})(\omega p\Delta\omega+\omega^2)}\frac{1}{N}\frac{\sin(\frac{\xi_{\mathrm{in}}}{2}(\omega p\Delta\omega+\omega^2))}{\sin(\frac{\xi_{\mathrm{in}}}{2N}(\omega p\Delta\omega+\omega^2))}\frac{1}{1+j\mathcal{S}_T(\omega p\Delta\omega+\omega^2)}$$
$$+\mathrm{e}^{-j(\xi_{\mathrm{pre}}+\frac{N-1}{2}\frac{\xi_{\mathrm{in}}}{N})(\omega p\Delta\omega)}\frac{1}{N}\frac{\sin(\frac{\xi_{\mathrm{in}}}{2}(\omega p\Delta\omega))}{\sin(\frac{\xi_{\mathrm{in}}}{2N}(\omega p\Delta\omega))}\frac{1}{1+j\mathcal{S}_T(\omega p\Delta\omega)}.$$

Long but straightforward calculations show that the pump intensity-modulation to probe intensity-modulation (IM-IM) filter for a long-haul terrestrial system is identical to the one "heuristically" derived by integrating all the infinitesimal contributions accounting for the IM-IM pump distortion from input to any point z, then generation of XPM at z, followed by the PM-IM conversion up to link end, as done in [33,34], which improved on a previous simpler approach [24,23,35]. The LP1-based filter expressions (21) are new, and have been obtained as a natural extension of the nonperiodic DM-NLSE to the WDM case. The filter expressions are most general, since they depend on the DM kernel $\eta(w)$, and thus they can be quickly and explicitly recomputed for any desired DM link configuration.

8. Conclusions

In this article we have provided a single analytical framework able to simply explain all major design rules developed for weakly-nonlinear optical DM systems, such as the heterogeneous terrestrial links employed in modern optical networks. Several results have been provided for the OOK modulation format, although the analysis could be extended to more advanced modulation formats.

Appendix A

Throughout the paper we use dimensionless units such as the map strength $\mathcal{S}_T$ and the in-line dispersion ξ_{in}. They relate to the standard dimensional units as:

$$\mathcal{S}_T \triangleq \frac{\lambda^2}{2\pi c}R^2\frac{1}{\alpha}D_T, \qquad \xi_{\mathrm{in}} \triangleq \frac{\lambda^2}{2\pi c}R^2 D_{\mathrm{in}}$$

where D_T [ps/nm/km] and α [m^{-1}] are the chromatic dispersion coefficient and the attenuation of the transmission fiber, respectively, D_{in} [ps/nm] is the in-line residual dispersion, c the speed of light and λ the channel wavelength. For a numerical feeling, a terrestrial link with Teralight$^{\mathrm{TM}}$ fiber ($D_T = 8$ ps/nm/km) at $R = 10$ Gb/s has a strength $\mathcal{S}_T = 0.022$. Since $\mathcal{S}_T$ scales as R^2, at 40 Gb/s the strength is 16 times larger, $\mathcal{S}_T \cong 0.35$. A value of $\xi_{\mathrm{in}} = 0.1$ corresponds to $D_{\mathrm{in}} = 800$ ps/nm at 10 Gb/s, while it decreases to 50 ps/nm at 40 Gb/s. The cumulated dispersions within the pre- and post-compensating fiber follow the same conversion rule as for ξ_{in}, namely: $\xi_{\mathrm{pre/post}} = \frac{\lambda^2}{2\pi c}R^2 D_{\mathrm{pre/post}}$, with $D_{\mathrm{pre/post}}$ in [ps/nm]. In terrestrial links with long spans and purely linear compensating fibers, the nonlinear phase cumulated by a signal of power P [mW] is from (2): $\Phi_{\mathrm{NL}} = NP\gamma/\alpha$, where γ [$\mathrm{m}^{-1}\,\mathrm{mW}^{-1}$] is the nonlinear coefficient of the transmission fiber.

Appendix B

Let u s now deal with the calculation of the integrals

$$U_1(0) = \int_{-\infty}^{\infty}\tilde{U}_1(\omega)\frac{\mathrm{d}\omega}{2\pi} \quad \text{and} \quad U_1^{(2)}(0) = -\int_{-\infty}^{\infty}\omega^2\tilde{U}_1(\omega)\frac{\mathrm{d}\omega}{2\pi}$$

The pulse Fourier transform is a real even function:

$$\tilde{U}_0(\omega) = \sqrt{2\pi}T_0\mathrm{e}^{-\frac{\omega^2T_0^2}{2}} = \sqrt{\frac{\pi d^2}{2}}\mathrm{e}^{-\frac{\omega^2d^2}{8}} \tag{B.1}$$

We now calculate the RP1 perturbation (3) as:

$$\tilde{U}_1(\omega) \triangleq \iint_{-\infty}^{\infty}\tilde{\eta}(\omega_1\omega_2)\tilde{U}_0(\omega)^3G(\omega,\omega_1,\omega_2)\frac{\mathrm{d}\omega_1}{2\pi}\frac{\mathrm{d}\omega_2}{2\pi}$$

where we defined $G(\omega,\omega_1,\omega_2)\triangleq \mathrm{e}^{-\frac{d^2}{4}(\omega_1^2+\omega_2^2+\omega_1\omega_2+2\omega(\omega_1+\omega_2))}$. Therefore the sought integrals become

$$U_1(0)=\iint_{-\infty}^{\infty}\tilde\eta(\omega_1\omega_2)\underbrace{\left[\int_{-\infty}^{\infty}\tilde U_0(\omega)^3\mathrm{e}^{-\frac{d^2}{2}(\omega_1+\omega_2)\omega}\frac{\mathrm{d}\omega}{2\pi}\right]}_{I_0}\mathrm{e}^{-\frac{d^2}{4}(\omega_1^2+\omega_2^2+\omega_1\omega_2)}\frac{\mathrm{d}\omega_1}{2\pi}\frac{\mathrm{d}\omega_2}{2\pi}$$

$$U_1^{(2)}(0)=-\iint_{-\infty}^{\infty}\tilde\eta(\omega_1\omega_2)\underbrace{\left[\int_{-\infty}^{\infty}\omega^2\tilde U_0(\omega)^3\mathrm{e}^{-\frac{d^2}{2}(\omega_1+\omega_2)\omega}\frac{\mathrm{d}\omega}{2\pi}\right]}_{I_2}\mathrm{e}^{-\frac{d^2}{4}(\omega_1^2+\omega_2^2+\omega_1\omega_2)}\frac{\mathrm{d}\omega_1}{2\pi}\frac{\mathrm{d}\omega_2}{2\pi}$$

with

$$I_0=\left(\frac{\pi d^2}{2}\right)^{\frac{3}{2}}\frac{1}{d}\sqrt{\frac{2}{3\pi}}\mathrm{e}^{\frac{d^2}{6}(\omega_1+\omega_2)^2}\quad\text{and}\quad I_2=\left(\frac{\pi d^2}{2}\right)^{\frac{3}{2}}\frac{4}{3d^3}\sqrt{\frac{2}{3\pi}}\left(1+\frac{d^2}{3}(\omega_1+\omega_2)^2\right)\mathrm{e}^{\frac{d^2}{6}(\omega_1+\omega_2)^2}$$

For long-span terrestrial systems, whose DM kernel is given in (5), the above integrals do not admit a closed form. However, at small strengths we can approximate $\tilde\eta_1(w)=\frac{1}{1+j\mathcal{S}_T w}\cong \mathrm{e}^{-j\mathcal{S}_T w}$. Since w plays the role of a squared pulsation ω^2, for the previous approximation to make sense we require that, over the main signal spectrum, obtained from (B.1) as $\pm\omega_0=\sqrt{\frac{8}{d^2}}$, the above approximation holds, i.e. we require that $\mathcal{S}_T\omega_0^2\ll 1$, i.e., $\mathcal{S}_T\ll 0.125d^2$. With such an approximation, the DM kernel becomes

$$\tilde\eta(w)\cong\frac{1}{N}\sum_{k=0}^{N-1}\mathrm{e}^{-j(\xi_{\mathrm{pre}}+\mathcal{S}_T+k\xi_s)w}$$

and thus integration yields the closed form expressions reported in (13).

Appendix C

In this appendix we derive the filters in (21).

C.1. Phase

Given the cosine component

$$m\cos(\omega_m t)=m\frac{\mathrm{e}^{j\omega_m t}+\mathrm{e}^{-j\omega_m t}}{2}$$

in the pump input amplitude modulation, we now look for the cosine component at frequency ω_m in the XPM-induced output phase. From (20) we have:

$$\theta_r^{\mathrm{XPM}}(t)\big|_{@\omega_m}=-\Phi_{\mathrm{NL}}\,\mathrm{Re}\big[m\mathrm{e}^{j\frac{\xi_{\mathrm{tot}}\omega_m^2}{2}}\big[H_p(\omega_m)\mathrm{e}^{j\omega_m t}+H_p(-\omega_m)\mathrm{e}^{-j\omega_m t}\big]\big]\tag{C.1}$$

and if we let $H_{\text{AM-PM}}(\omega)$ be the response of the amplitude-modulation to cross phase modulation (AM-PM) filter, then the above must also be

$$\theta_r^{\mathrm{XPM}}(t)\big|_{@\omega_m}=\frac{m}{2}\big[H_{\text{AM-PM}}(\omega_m)\mathrm{e}^{j\omega_m t}+H_{\text{AM-PM}}(-\omega_m)\mathrm{e}^{-j\omega_m t}\big]$$

Hence we rewrite (C.1) as

$$\begin{aligned}\theta_r^{\mathrm{XPM}}(t)\big|_{@\omega_m}=\frac{m}{2}(-\Phi_{\mathrm{NL}})\big[&\mathrm{e}^{j\frac{\xi_{\mathrm{tot}}\omega_m^2}{2}}\big[H_p(\omega_m)\mathrm{e}^{j\omega_m t}+H_p(-\omega_m)\mathrm{e}^{-j\omega_m t}\big]\\&+\mathrm{e}^{-j\frac{\xi_{\mathrm{tot}}\omega_m^2}{2}}\big[H_p^*(\omega_m)\mathrm{e}^{-j\omega_m t}+H_p^*(-\omega_m)\mathrm{e}^{j\omega_m t}\big]\big]\end{aligned}$$

from which we recognize that

$$H_{\text{AM-PM}}(\omega_m) = -\Phi_{\text{NL}}\big[\mathrm{e}^{j\frac{\xi_{\text{tot}}\omega_m^2}{2}} H_p(\omega_m) + \mathrm{e}^{-j\frac{\xi_{\text{tot}}\omega_m^2}{2}} H_p^*(-\omega_m)\big]$$

Now, for small modulation index m, the intensity of the input modulated signal is $|A_{r0}(L,t)|^2 \cong 1 + 2m\cos(\omega_m t)$, so that the IM-PM filter, relating the input intensity modulation (IM) to the output cross-phase modulation, is half of the above AM-PM filter. This leads to the first filter in (21).

C.2. Intensity

We now look for the cosine component at frequency ω_m in the XPM-induced output RID. From (20) we get:

$$\begin{aligned}\Delta I_r^{\text{XPM}}(t)\big|_{@\omega_m} &= -1 + \exp\big\{2m\Phi_{\text{NL}}\,\text{Im}\big[\mathrm{e}^{j\frac{\xi_{\text{tot}}\omega_m^2}{2}}\big[H_p(\omega_m)\mathrm{e}^{j\omega_m t} + H_p(-\omega_m)\mathrm{e}^{-j\omega_m t}\big]\big]\big\}\\ &\cong 2m\Phi_{\text{NL}}\,\text{Im}\big[\mathrm{e}^{j\frac{\xi_{\text{tot}}\omega_m^2}{2}}\big[H_p(\omega_m)\mathrm{e}^{j\omega_m t} + H_p(-\omega_m)\mathrm{e}^{-j\omega_m t}\big]\big] \qquad \text{(C.2)}\end{aligned}$$

where in the second line we linearized the exponential assuming a small m. If we let $H_{\text{AM-IM}}(\omega)$ be the response of the AM-IM filter, then the above must also be

$$\Delta I_r^{\text{XPM}}(t)\big|_{@\omega_m} = \frac{m}{2}\big[H_{\text{AM-IM}}(\omega_m)\mathrm{e}^{j\omega_m t} + H_{\text{AM-IM}}(-\omega_m)\mathrm{e}^{-j\omega_m t}\big].$$

Hence we rewrite (C.2) as

$$\begin{aligned}\Delta I_r^{\text{XPM}}(t)\big|_{@\omega_m} = \frac{m}{2j}(2\Phi_{\text{NL}})\big[&\mathrm{e}^{j\frac{\xi_{\text{tot}}\omega_m^2}{2}}\big[H_p(\omega_m)\mathrm{e}^{j\omega_m t} + H_p(-\omega_m)\mathrm{e}^{-j\omega_m t}\big]\\ &- \mathrm{e}^{-j\frac{\xi_{\text{tot}}\omega_m^2}{2}}\big[H_p^*(\omega_m)\mathrm{e}^{-j\omega_m t} + H_p^*(-\omega_m)\mathrm{e}^{j\omega_m t}\big]\big]\end{aligned}$$

from which we recognize that

$$H_{\text{AM-IM}}(\omega_m) = -j2\Phi_{\text{NL}}\big[\mathrm{e}^{j\frac{\xi_{\text{tot}}\omega_m^2}{2}} H_p(\omega_m) - \mathrm{e}^{-j\frac{\xi_{\text{tot}}\omega_m^2}{2}} H_p^*(-\omega_m)\big]$$

so that the IM-IM filter, relating the input intensity modulation to the output relative intensity distortion, is half of the above AM-IM filter.

References

[1] I.P. Kaminow, T.L. Koch (Eds.), Optical Fiber Telecommunications, vol. IIIA, Academic, 1997 (Chapter 8).
[2] S. Bigo, Y. Frignac, J.-C. Antona, G. Charlet, S. Lanne, C. R. Physique 4 (2003) 105–113.
[3] A. Cauvin, Y. Frignac, S. Bigo, in: Proc. European Conf. Opt. Commun. ECOC '03, Rimini, Italy, paper Mo4.2.4.
[4] J.-C. Antona, S. Bigo, in: Proc. Optical Fiber Commun. Conf. OFC '02, Anaheim, CA, paper WX5.
[5] A. Cauvin, Y. Frignac, S. Bigo, Electron. Lett. 39 (23) (2003) 1670–1671.
[6] R.I. Killey, H.J. Thiele, V. Mikhailov, P. Bayvel, IEEE Photon. Technol. Lett. 12 (2000) 1624–1626.
[7] Y. Frignac, J.-C. Antona, S. Bigo, J.-P. Hamaide, in: Proc. OFC '02, Anaheim, CA, pp. 612–613, paper ThFF5.
[8] Y. Frignac, J.-C. Antona, S. Bigo, Proc. OFC '04, Los Angeles, CA, paper TuN3.
[9] D. Marcuse, J. Lightw. Technol. 9 (1) (1991) 121–128.
[10] H.A. Haus, J. Opt. Soc. Am. B, Opt. Phys. 8 (5) (1991) 1122–1126.
[11] L.F. Mollenauer, S.G. Evangelides, H.A. Haus, J. Lightw. Technol. 9 (2) (1991) 194–196.
[12] I.R. Gabitov, S.K. Turitsyn, Opt. Lett. 21 (1996) 327–329.
[13] C. Paré, P.-B. Bélanger, Opt. Lett. 25 (2000) 881–883.
[14] X. Wei, Opt. Lett. 31 (17) (2006) 2544–2546.
[15] M.J. Ablowitz, T. Hirooka, J. Opt. Soc. Am. B, Opt. Phys. 19 (2002) 425–439.
[16] M.J. Ablowitz, T. Hirooka, IEEE J. Sel. Topics Quantum Electron. 8 (2002) 603–615.
[17] H. Louchet, A. Hodzic, K. Petermann, A. Robinson, IEEE Photon. Technol. Lett. 17 (2005) 247–249.
[18] H. Louchet, A. Hodzic, K. Petermann, A. Robinson, R. Epworth, IEEE Photon. Technol. Lett. 17 (2005) 2089–2091.
[19] E. Ciaramella, E. Forestieri, IEEE Photon. Technol. Lett. 17 (2005) 91–93.
[20] E. Forestieri, M. Secondini, Solving the nonlinear Schroedinger equation, in: E. Forestieri (Ed.), Optical Communication Theory and Techniques, Springer, 2005, pp. 3–11.
[21] P. Johannisson, J. Opt. Soc. Am. B 24 (4) (2007) 729–738.

[22] I.P. Kaminow, T. Li (Eds.), Optical Fiber Telecommunications, vol. IVB, Elsevier, 2002 (Chapter 6).
[23] A. Cartaxo, IEEE J. Lightw. Technol. 17 (1999) 178–190.
[24] G. Bellotti, M. Varani, C. Francia, A. Bononi, IEEE Photon. Technol. Lett. 10 (1998) 1745–1747.
[25] G.P. Agrawal, Nonlinear Fiber Optics, second ed., Academic, 1995.
[26] A. Vannucci, P. Serena, A. Bononi, IEEE J. Lightw. Technol. 20 (2002) 1102–1112.
[27] B. Xu, M. Brandt-Pearce, IEEE Photon. Technol. Lett. 14 (2002) 47–49.
[28] P. Minzioni, A. Schiffini, Optics Express 13 (21) (2005) 8460–8468.
[29] A. Mecozzi, C.B. Clausen, M. Shtaif, IEEE Photon. Technol. Lett. 12 (2000) 1633–1635.
[30] A. Papoulis, Probability, Random Variables, and Stochastic Processes, third ed., McGraw-Hill Int. Ed., 1991.
[31] A. Bononi, P. Serena, A. Orlandini, A unified design framework for single-channel dispersion-managed terrestrial systems, IEEE J. Lightw. Technol. (2008), in press.
[32] A. Papoulis, J. Opt. Soc. Am. A 11 (1) (1994) 3–13.
[33] M. Varani, G. Bellotti, A. Bononi, C. Francia, in: Proc. Lasers Electro-Opt. Soc. LEOS '98, Orlando, FL, December 1998, pp. 376–377.
[34] A. Bononi, G. Bellotti, M. Varani, C. Francia, SPM/XPM-induced intensity distortion in WDM systems, in: A. Bononi (Ed.), Optical Networking, Springer, 1999, pp. 383–398.
[35] R. Killey, H.J. Thiele, V. Mikhailov, P. Bayvel, IEEE Photon. Technol. Lett. 12 (2000) 804–806.